# A NOVEL FRACTIONAL ORDER DERIVATE BASED LOG-DEMONS WITH DRIVING FORCE FOR HIGH ACCURATE IMAGE REGISTRATION

*Cheng Xu*[1], *Ying Wen*[1]*, *Bing He*[2]

1. Department of Computer Science and Technology,
East China Normal University, Shanghai, China.
2. Shanghai Inspection & Maintenance of Power Company, Shanghai, China.

## ABSTRACT

Image registration methods based on Thirion's demons method update displacement field by the image gradient obtained by integer order derivate. However, the fractional order derivate is superior to integral order derivate for computing image gradient under weak texture or smooth regions. To obtain high accurate image registration, we propose a new fractional order derivate based Log-Demons with driving force. We design a new fractional order derivate convolution mask based on Grünwald-Letnikov (GL) definition to get accurate image gradient. Then, we integrate fractional order derivate into Log-Demons with driving force. The experiments on synthetic and MRI brain images validate that the use of fractional order derivate to compute gradient not only improves the registration accuracy but also speeds up the registration process.

***Index Terms*—** Image registration, image gradient, fractional order derivate, convolution mask

## 1. INTRODUCTION

Nonrigid image registration is one of fundamental fields in computer vision, especially for medical image processing. Owning to the pioneering research of Thirion's basic demons algorithm [1], which introduced diffusing model into image registration, abundant relevant work is devoted to improving the performance of demons algorithm over the past decades [2],[3],[4]. But these improved methods have a limitation that they do not maintain the invertibility of the displacement fields. Log-Demons was proposed by Vercauteren *et al.* [5],[6],[7] to produce diffeomorphic transformation in Lie Group. Based on Log-Demons, Lorenzi *et al.* [8] proposed a robust registration method named LCC-Demons which used local correlation coefficient as similarity metric. The approaches under Log-Demons employed graph spectrum [9] and Spectral Graph Wavelets [10] to cast registration into a feature matching problem and they obtained an improvement in registration accuracy.

However, for these variants of demons algorithm, the force to update the displacement field is typically provided by image gradient and it will be prone to local minima when image gradient is null in textureless areas [9]. The conventional way of calculating the gradient is to use integer order derivate, and thus the gradient magnitude in weak texture is approximately zero. Fortunately, it is reported in [11] that fractional order derivate can enhance image gradient in smooth area, which is often used in texture enhancement [12]. After that, Zhang *et .al* [13] integrated fractional order derivate into variational model to produce accurate and smooth deformation fields. Melbourne *et al.* [14] implemented registration by fractional gradient images instead of intensity images and the result shows better recovery.

In this paper, we propose a novel fractional order derivate based Log-Demons with driving force for high accurate image registration. We construct fractional order derivate convolution masks to convolve with image to obtain image gradient and then embed it into Log-Demons with driving force [15]. This can enhance gradient magnitude in smooth or weak texture regions, thus the updated displacement fields are more accurate. We evaluate our proposed method on synthetic and MRI brain images and the experimental results validate that our method is effective.

## 2. METHOD

Log-Demons with driving force is proposed by Zhang *et .al* [15], which can obtain a good result for the large deformation image registration. We call it DLog-Demons here. To further obtain high accuracy of DLog-Demons, we propose a novel fractional order derivate based DLog-Demons.

### 2.1. Fractional order Derivate based DLog-Demons

Given a fixed image $F$ and a moving image $M$, the goal of image registration is to seek a displacement field $s(.) : p \to s(p)$ for each pixel $p$ that makes $F(p)$ and $M(s(p))$ are similar.

This work was supported by National Nature Science Foundation of China (No.61773166), Natural Science Foundation of Shanghai (No.17ZR1408200) and the Science and Technology Commission of Shanghai Municipality under research grant (No.14DZ2260800).

*Corresponding author email: ywen@cs.ecnu.edu.cn

The main point of DLog-Demons is the use of driving force. The driving force $u^c$ is defined by the correspondent boundary points between fixed and moving images. Then $u^c$ is integrated into Log-Demons [7] by exponential map $\exp(\cdot)$, the energy function of DLog-Demons is as followed:

$$E(u) = \frac{1}{\lambda_i^2}\mathrm{Sim}(F, M \circ s \circ \exp(u) \circ \exp(\frac{1}{\lambda_k^2}u^c)) + \frac{1}{\lambda_x^2}\mathrm{dist}(s, s \circ \exp(u) \circ \exp(\frac{1}{\lambda_k^2}u^c)) + \frac{1}{\lambda_T^2}\mathrm{Reg}(s) \quad (1)$$

where $\lambda_i$, $\lambda_x$ and $\lambda_T$ are the noise on image intensity, a spatial uncertain on the correspondences and the amount of regularization, respectively. $\lambda_k$ controls the amount of driving force. The formula of the updated displacement field $u$ at each pixel $p$ can be obtained by optimizing Eq.1 with the first order polynomial approximation [15]:

$$u(p) = -\frac{F(p) - M \circ s(p)}{||J_p||^2 + \frac{\lambda_i^2(p)}{\lambda_x^2}} J_p^T - \frac{1}{\lambda_k^2}u^c(p) \quad (2)$$

Different experssion of $J^p$ in Eq.2 can be explained by adopting different optimization strategies [7]. Based on the Gauss-Newton scheme, $J_p = -\nabla_p(M \circ s)$.

In general, conventional integral order derivate is hard to capture the gradient in smooth regions where gray scale changes gently, however, fractional order derivate is sentive to weak texture regions. This allows us to propose fractional order derivate mask $H$ to convolve with image to get gradient, namely $J_p = H * (M \circ s)_p$. Thus, the update rule of the proposed method is:

$$u(p) = -\frac{(F(p) - M \circ s(p))(H * (M \circ s)_p^T)}{||H * (M \circ s)_p||^2 + \frac{\lambda_i^2(p)}{\lambda_x^2}} - \frac{1}{\lambda_k^2}u^c(p) \quad (3)$$

Eq.3 is our proposed rule to update displacement field. Due to fractional order derivate embedded, image gradient in weak texture or smooth regions can be enhanced. Thus, high accurate updated displacement field can be obtained. We call our method FDLog-Demons. We will present how to construct the fractional order derivate mask $H$ in the following sections.

### 2.2. Fractional Order Derivative

The fractional order derivate has a long history and three classical fractional order derivates have been widely applied in image processing, namely Grünwald-Letnikov (GL), Riemann–Liouville (RL) and Caputo [16]. The GL definition derives from the preceding of integer order derivate and is the limit of the weighted sum, thus it has an advantage in numerical calculation. Given a one dimension signal $f(x)$ in domain $[a, x], a < x, a \in \mathrm{R}, x \in \mathrm{R}$, $h$ is the step size and $\alpha \in \mathrm{R}$ denotes an arbitrary fractional order, the GL derivative is defined by:

$$^{GL}D_{[a,x]}^{\alpha} f(x) = \lim_{h \to 0} h^{-\alpha} \sum_{k=0}^{n=[\frac{x-a}{h}]} (-1)^k C_\alpha^k f(x - kh) \quad (4)$$

where $C_\alpha^k$ is the binomial coefficient. In 1D computational domain, we can divide the domain $[a, x]$ by the interval $h = 1$, then a discrete formulation of $f(x)$ can be obtained:

$$\begin{aligned} \frac{\mathrm{d}^\alpha f(x)}{\mathrm{d}x^\alpha} \approx & f(x) - \alpha f(x-1) + \frac{\alpha^2 - \alpha}{2} f(x-2) \\ & + \frac{-\alpha^3 + 3\alpha^2 - 2\alpha}{6} f(x-3) + \cdots \\ & + \frac{-\alpha(-\alpha+1)\cdots(-\alpha+n-1)}{n!} f(x-n) \end{aligned} \quad (5)$$

### 2.3. Construction of Fractional Order Derivate Mask

Images are usually treated as 2D computational domains, thus we need to transform Eq.5 to 2D fractional order derivative. For an arbitrary pixel $f(x, y)$ in an image, the fractional order derivative of negative $x$ direction under GL definition is given as:

$$\begin{aligned} \frac{\partial^\alpha f(x, y)}{\partial x_-^\alpha} \approx & f(x, y) - \alpha f(x-1, y) + \frac{\alpha^2 - \alpha}{2} f(x-2, y) \\ & + \frac{-\alpha^3 + 3\alpha^2 - 2\alpha}{6} f(x-3, y) + \cdots \\ & + \frac{-\alpha(-\alpha+1)\cdots(-\alpha+n-1)}{n!} f(x-n, y) \end{aligned} \quad (6)$$

The fractional order derivative of negative $y$ direction is similar to that of negative $x$-direction.

According to the research of Pu *et al.* [17], the preservation magnitude of image gradient in weak texture and smooth regions by fractional order derivate is superior to that by integer order derivate. From our point of view, the first two items in Eq.6 have the similar effect as the integer order derivate with respect to gradient since the structure of them are similar to integer order derivate. The difference between fractional order derivate and integer order derivate is that there are high order expansion items in the former. The high order expansion items are more sensitive to slight change of gray scale in smooth and textureless regions. Hence, these high order expansion items can enhance image gradient in textureless and smooth regions to some extend and we can select them to compute image gradient. For numerical completion, we perform spatial convolution with the image. Fig.1 shows our constructed convolution masks $H_x$ and $H_y$ on $x$ and $y$ direction, respectively. Balancing robustness with the computational complexity, we set our fractional order derivate masks on $x$ and $y$ direction to a fixed size $5 \times 5$. We choose the coefficients of the third and fourth items in Eq.6 as mask coefficients. Then we employ the constructed masks to convolve with the image. The convolution result is regarded as image gradient and it can distinguish textureless and smooth regions from image. Similar to Sobel operator [18], we use the weight 4 to highlight the role of the pixel at the center of the mask. Then as is shown in Eq.3, we obtain the update rule of our proposed method.

|  |  |  |  |  |
|---|---|---|---|---|
| $\frac{\psi_1}{48}$ | $\frac{\psi_2}{16}$ | 0 | $-\frac{\psi_2}{16}$ | $-\frac{\psi_1}{48}$ |
| $\frac{\psi_1}{24}$ | $\frac{\psi_2}{8}$ | 0 | $-\frac{\psi_2}{8}$ | $-\frac{\psi_1}{24}$ |
| $\frac{\psi_1}{6}$ | $\frac{\psi_2}{2}$ | 0 | $-\frac{\psi_2}{2}$ | $-\frac{\psi_1}{6}$ |
| $\frac{\psi_1}{24}$ | $\frac{\psi_2}{8}$ | 0 | $-\frac{\psi_2}{8}$ | $-\frac{\psi_1}{24}$ |
| $\frac{\psi_1}{48}$ | $\frac{\psi_2}{16}$ | 0 | $-\frac{\psi_2}{16}$ | $-\frac{\psi_1}{48}$ |

(a) $x$ direction mask, $H_x$

|  |  |  |  |  |
|---|---|---|---|---|
| $\frac{\psi_1}{48}$ | $\frac{\psi_1}{24}$ | $\frac{\psi_1}{6}$ | $\frac{\psi_1}{24}$ | $\frac{\psi_1}{48}$ |
| $\frac{\psi_2}{16}$ | $\frac{\psi_2}{8}$ | $\frac{\psi_2}{2}$ | $\frac{\psi_2}{8}$ | $\frac{\psi_2}{16}$ |
| 0 | 0 | 0 | 0 | 0 |
| $-\frac{\psi_2}{16}$ | $-\frac{\psi_2}{8}$ | $-\frac{\psi_2}{2}$ | $-\frac{\psi_2}{8}$ | $-\frac{\psi_2}{16}$ |
| $-\frac{\psi_1}{48}$ | $-\frac{\psi_1}{24}$ | $-\frac{\psi_1}{6}$ | $-\frac{\psi_1}{24}$ | $-\frac{\psi_1}{48}$ |

(b) $y$ direction mask, $H_y$

**Fig. 1**. Our proposed fractional order derivate mask $H$ on $x$ and $y$ direction, respectively. $\psi_1 = -\alpha^3 + 3\alpha^2 - 2\alpha$, $\psi_2 = \alpha^2 - \alpha$.

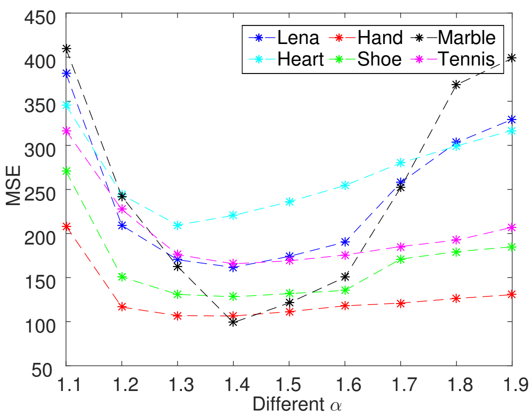


**Fig. 2**. The performance of FDLog-Demons under different fractional order $\alpha$ on synthetic images.

## 3. EXPERIMENTS

We evaluate the performance of our approach on synthetic images and MRI brain images and compare our method with original Log-Demons [7] and DLog-Demons [15]. For empirical parameter settings, we use the same parameters for the compared methods $\{\lambda_i, \lambda_x\} = \{1, 2\}$. The number of iterations is set to 100. We utilize the Mean Square Error (MSE) and the Relative Sum of Squared Difference (Rel.SSD) [19] to measure registration quality.

### 3.1. Experiments on Synthetic Images

To show the effectiveness of our proposed method, we firstly select synthetic images from [15] to test. The first and second columns in Fig.3 show some synthetic images and the corresponding moving images are obtained by randomly large non-rigid deformations, respectively.

#### *3.1.1. Analysis on Fractional Order $\alpha$*

From Eq.3 and Fig.1, we can see that the performance of the proposed FDLog-Demons depends on the value of $\alpha$. Some

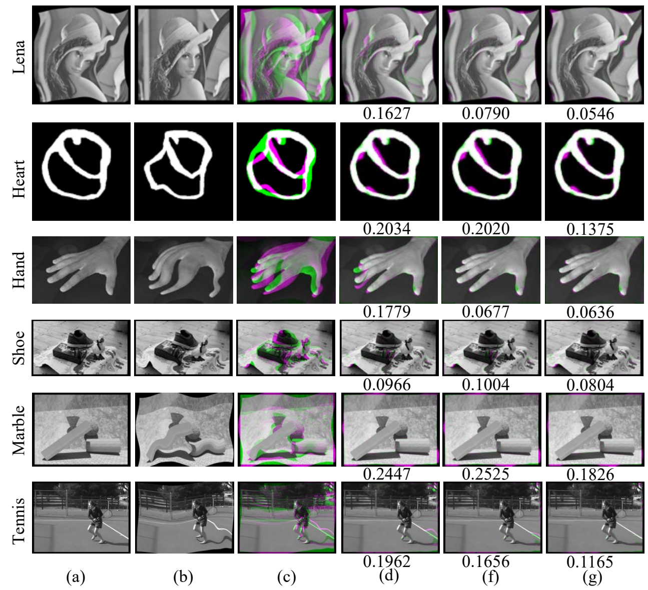


**Fig. 3**. Example of registration results on synthetic images. (a)(b) are fixed and moving images. (c) is the fusion fixed and moving images. The area of green and purple stands for initial difference. (d)(e)(f) are the Rel.SSD and the difference of fixed image with results aligned by Log-Demons, DLog-Demons and our proposed FDLog-Demons, respectively.

synthetic images [15] are used to detect the optimal $\alpha$. Fig.2 studies the performance of FDLog-Demons under different fractional order $\alpha$. From the experiments, we find that the results are better when $\alpha > 1$. For different images, we can see that the MSE first drops and then raises up with the increase of $\alpha$. Fig.2 shows that the best fractional order $\alpha$ is about 1.4. Thus, we set $\alpha$ to 1.4 in the following experiments.

#### *3.1.2. Results on Synthetic Images*

To validate the performance of our method, we compare it with Log-Demons [7] and DLog-Demons [15] and the registration results are shown in Fig.3. We can see that large deformations exist in all images from Fig.3(c). For Lena, the results of Log-Demons and DLog-Demons have large difference in hair region. In contrast, our method registers Lena's hair successfully. Although gray scale changes slightly in hair region, the gradient in this region computed by our method is more accurate because fractional order derivate is easy to capture the change of gray value. The same result is shown in the upper right corner of the box in shoe. For heart and hand, our proposed method has less difference in the edge of heart and finger. For marble, it is difficult to see obvious difference from vision, but the MSE of our method is reduced by 25.38% and 38.3% compared with the other two methods. For tennis, it is difficult to align the twisted line in the bottom right corner. Log-Demons fails to align and DLog-

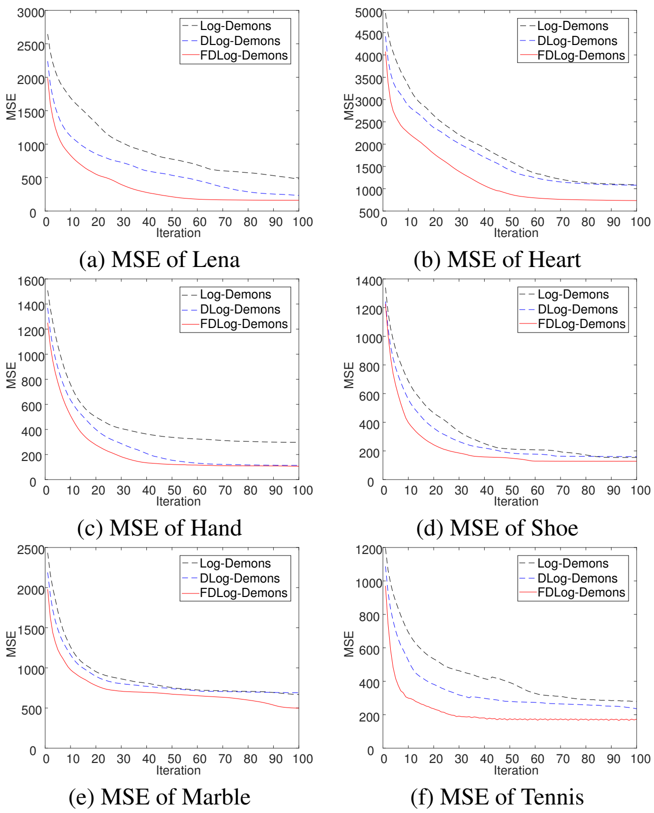


(a) MSE of Lena (b) MSE of Heart

(c) MSE of Hand (d) MSE of Shoe

(e) MSE of Marble (f) MSE of Tennis

**Fig. 4**. Comparison of three methods by MSE curves of synthetic images.

Demons has a slight improvement than Log-Demons, while our method aligns the twisted line well. The results of experiment on synthetic images show our method can obtain excellent performance.

Fig.4 shows the MSE curves of synthetic images. For the above six synthetic experiments, the MSE curves of our method drop more rapidly than Log-Demons and DLog-Demosn, especially at the beginning of registration process. It shows fractional order derivate can accelerate the registration process which means the registration process is easier to converge. In other words, our method can obtain high registration accuracy within fewer iterations. The results demonstrate the effectiveness of fractional order derivate embedded in DLog-Demons.

### 3.2. Experiments on MRI Brain Images

Demons based image registration methods are mainly applied in medical image processing. We randomly select 45 pairs of T1 images from BrainWeb [20] as fixed and moving images, respectively. Non-brain tissues are preprocessed by the brain extraction tool (BET) [21]. Similar to the experiments in [22], we deform the original moving images by 25, 50 and 75 pixels to generate largely deformable images, respectively. Thus, we complete four groups of experiments to test our proposed method.

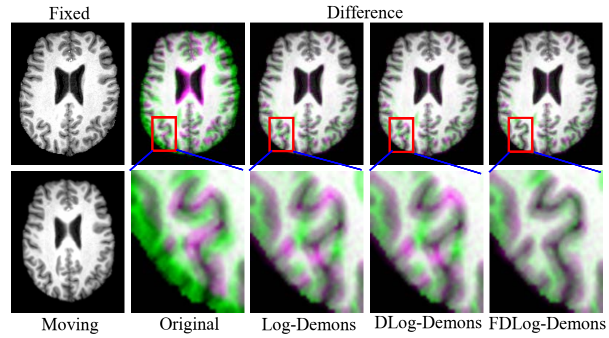


**Fig. 5**. A comparison of three methods on T1 brain images from BrainWeb [20].

**Table 1**. Comparison of registration results on MRI brain images.

| **Group / pixel deformed** | **Average MSE / Rel.SSD** | | |
|---|---|---|---|
| | Log-Demons | DLog-Demons | FDLog-Demons |
| 1 / 0 pixel | 567.53 / 0.1999 | 566.14 / 0.1992 | **559.58 / 0.1969** |
| 2 / 25 pixels | 578.64 / 0.2049 | 577.87 / 0.2047 | **569.35 / 0.2018** |
| 3 / 50 pixels | 626.35 / 0.2107 | 626.12 / 0.2105 | **615.54 / 0.2071** |
| 4 / 75 pixels | 739.36 / 0.2286 | 728.68 / 0.2253 | **714.45 / 0.2211** |

Fig.5 shows an example of T1 brain image registration. The images in the first column are fixed image (top) and moving image (below). The images in the rest columns are the difference and their local enlargement images, which are obtained by the original difference, difference between the fixed image and Log-Demons, DLog-Demons and FDLog-Demons, respectively. We can see that our proposed method has lower difference than Log-Demons and DLog-Demons in regions marked by red rectangles. Table 1 shows the average MSE and Rel.SSD of our proposed FDLog-Demons compared to Log-Demons and DLog-Demons. It can be seen that our proposed method obtains better results than Log-Demons and DLog-Demons in terms of the average MSE and Rel.SSD. It shows that our method is superior to other methods and can obtain high accuracy for image registration.

## 4. CONCLUSION

This paper presents a novel fractional order derivate based DLog-Demons for high accurate image registration. In this method, we design a new fractional order derivate mask to compute image gradient in place of integer order derivate to update the displacement field. We integrate the new fractional order derivate into DLog-Demons to obtain high registration accuracy. The experimental results show that our proposed approach can obtain competitive registration accuracy and also can speed up the registration process.

## 5. REFERENCES


[1] J. Thirion, "Image matching as a diffusion process: an analogy with maxwell's demons," *Medical image analysis*, vol. 2, no. 3, pp. 243–260, 1998.

[2] H. Wang, L. Dong, J. O'Daniel, R. Mohan, et al., "Validation of an accelerated 'demons' algorithm for deformable image registration in radiation therapy," *Physics in Medicine & Biology*, vol. 50, no. 12, pp. 2887, 2005.

[3] N. Cahill, J. Noble, and D. Hawkes, "A demons algorithm for image registration with locally adaptive regularization," in *International Conference on Medical Image Computing and Computer-Assisted Intervention*. Springer, 2009, pp. 574–581.

[4] E. Hwuang, S. Danish, M. Rusu, et al., "Anisotropic smoothing regularization (ansr) in thirion's demons registration evaluates brain mri tissue changes post-laser ablation," in *Engineering in Medicine and Biology Society (EMBC)*. IEEE, 2013, pp. 4006–4009.

[5] T. Vercauteren, X. Pennec, A. Perchant, and N. Ayache, "Non-parametric diffeomorphic image registration with the demons algorithm," in *International Conference on Medical Image Computing and Computer-Assisted Intervention*. Springer, 2007, pp. 319–326.

[6] T. Vercauteren, X. Pennec, A. Perchant, and N. Ayache, "Symmetric log-domain diffeomorphic registration: A demons-based approach," in *International conference on medical image computing and computer-assisted intervention*. Springer, 2008, pp. 754–761.

[7] T. Vercauteren, X. Pennec, A. Perchant, and N. Ayache, "Diffeomorphic demons: Efficient non-parametric image registration," *NeuroImage*, vol. 45, no. 1, pp. S61–S72, 2009.

[8] M. Lorenzi, N. Ayache, G. Frisoni, et al., "Lcc-demons: a robust and accurate symmetric diffeomorphic registration algorithm," *NeuroImage*, vol. 81, pp. 470–483, 2013.

[9] H. Lombaert, L. Grady, X. Pennec, et al., "Spectral log-demons: diffeomorphic image registration with very large deformations," *International journal of computer vision*, vol. 107, no. 3, pp. 254–271, 2014.

[10] N. Pham, D. Helbert, P. Bourdon, and P. Carré, "Spectral graph wavelet based nonrigid image registration," in *IEEE International Conference on Image Processing*. IEEE, 2018, pp. 3348–3352.

[11] Q. Yang, D. Chen, T. Zhao, and Y. Chen, "Fractional calculus in image processing: a review," *Fractional Calculus and Applied Analysis*, vol. 19, no. 5, pp. 1222–1249, 2016.

[12] J. Guan, J. Ou, Z. Lai, and Y. Lai, "Medical image enhancement method based on the fractional order derivative and the directional derivative," *International Journal of Pattern Recognition and Artificial Intelligence*, vol. 32, no. 03, pp. 1857001, 2018.

[13] J. Zhang and K. Chen, "Variational image registration by a total fractional-order variation model," *Journal of Computational Physics*, vol. 293, pp. 442–461, 2015.

[14] A. Melbourne, N. Cahill, C. Tanner, et al., "Using fractional gradient information in non-rigid image registration: application to breast mri," in *Medical Imaging 2012: Image Processing*. International Society for Optics and Photonics, 2012, vol. 8314, p. 83141Z.

[15] L. Zhang and Y. Wen, "Log-demons with driving force for large deformation image registration," in *International Joint Conference on Neural Networks*. IEEE, 2016, pp. 3052–3059.

[16] I. Podlubny, *Fractional differential equations: an introduction to fractional derivatives, fractional differential equations, to methods of their solution and some of their applications*, vol. 198, Elsevier, 1998.

[17] Y. Pu, J. Zhou, and X. Yuan, "Fractional differential mask: a fractional differential-based approach for multiscale texture enhancement," *IEEE transactions on image processing*, vol. 19, no. 2, pp. 491–511, 2010.

[18] I. Sobel, "Camera models and machine perception," Tech. Rep., Computer Science Department, Technion, 1972.

[19] N. Chumchob, K. Chen, and C. Brito-Loeza, "A fourth-order variational image registration model and its fast multigrid algorithm," *Multiscale Modeling & Simulation*, vol. 9, no. 1, pp. 89–128, 2011.

[20] C. Cocosco, V. Kollokian, R. Kwan, G. Pike, and A. Evans, "Brainweb: Online interface to a 3d mri simulated brain database," in *NeuroImage*. Citeseer, 1997.

[21] M. Jenkinson, M. Pechaud, S. Smith, et al., "Bet2: Mr-based estimation of brain, skull and scalp surfaces," in *Eleventh annual meeting of the organization for human brain mapping*. Toronto., 2005, vol. 17, p. 167.

[22] B. Mishra, U. Pati, and U. Sinha, "Modified demons registration for highly deformed medical images," in *International Conference on Image Information Processing*. IEEE, 2015, pp. 152–156.